Journal of Medicinal Chemistry

Article

Urotensin-II Receptor Ligands. From Agonist to Antagonist Activity

Paolo Grieco, Alfonso Carotenuto, Pietro Campiglia, Luciana Marinelli, Teresa Lama, Riccardo Patacchini, Paolo Santicioli, Carlo A. Maggi, Paolo Rovero, and Ettore Novellino

J. Med. Chem., **2005**, 48 (23), 7290-7297• DOI: 10.1021/jm058043j • Publication Date (Web): 14 October 2005

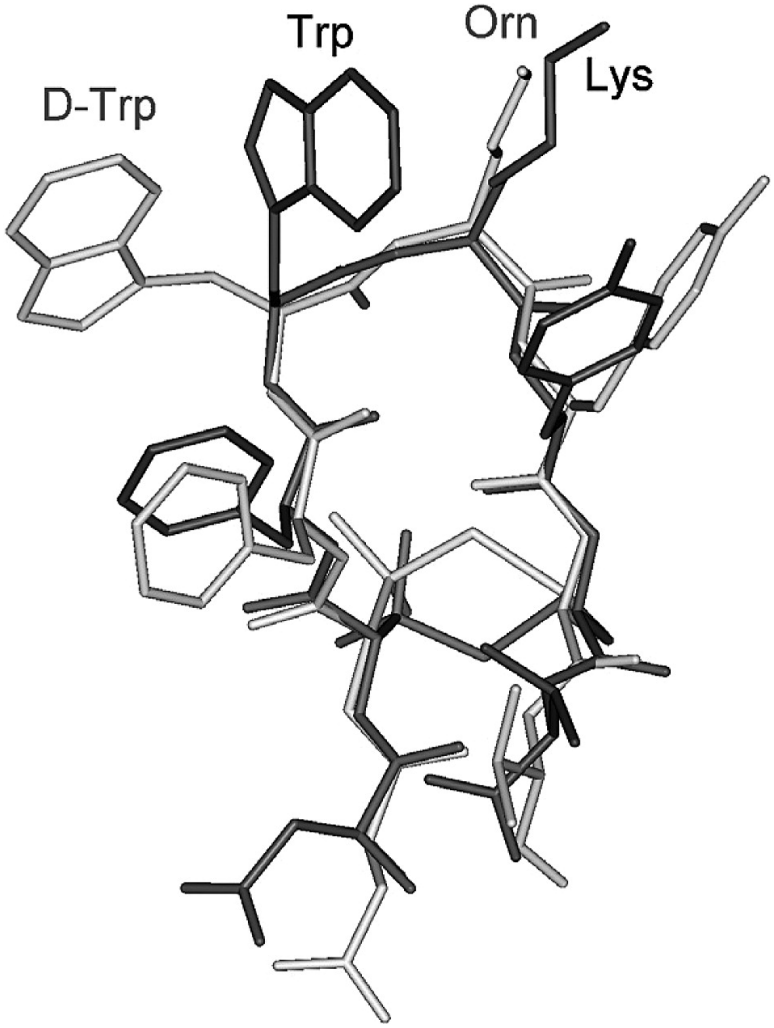

Urotensin-II Receptor Ligands. From Agonist to Antagonist Activity

Paolo Grieco,[§,‡] Alfonso Carotenuto,[§,‡] Pietro Campiglia,[§] Luciana Marinelli,[§] Teresa Lama,[§] Riccardo Patacchini,[†] Paolo Santicioli,[||] Carlo A. Maggi,[||] Paolo Rovero,[#] and Ettore Novellino*[,§]

Department of Pharmaceutical and Toxicological Chemistry, University of Naples "Federico II", I-80131 Naples, Italy, Laboratorio Interdipartimentale di Chimica e Biologia dei Peptidi e Proteine, Dipartimento di Scienze Farmaceutiche, Università di Firenze, I-50019 Sesto Fiorentino, Florence, Italy, Department of Pharmacology, Chiesi Pharmaceuticals S.p.A., Via Palermo 26/A, I-43100 Parma, Italy, and Department of Pharmacology, Menarini Ricerche, Via Rismondo 12/A, I-50131, Florence, Italy

Received July 25, 2005

Urotensin II (U-II) is a disulfide bridged peptide hormone recently identified as the ligand of a G-protein-coupled receptor. Human U-II (H-Glu-Thr-Pro-Asp-cyclo[Cys-Phe-Trp-Lys-Tyr-Cys]-Val-OH) has been described as the most potent vasoconstrictor compound identified to date. We have recently identified both a superagonist of hU-II termed P5U and the compound termed urantide, which is the most potent UT receptor peptide antagonist described to date. Our previous conformational studies showed that hU-II and its analogues with agonist activity adopt a well-defined type II′ β-hairpin structure in anisotropic SDS membrane-like environment. This structural arrangement allows tight contact among the Trp[7], Lys[8], and Tyr[9] side chains, which is fundamental to obtain full agonist activity. Here, we report an extensive SAR study on new analogues with agonist/antagonist activity on UT receptor. We investigated their biological activity and performed a conformational analysis by spectroscopic and computational methods. Our goal is to obtain a structure-based model able to explain the agonist/antagonist functional switching of these ligands.

Introduction

Urotensin-II (U-II) is a cyclic peptide originally isolated from goby fish urophysis.[1] Recently, U-II was identified as the natural ligand of an orphan G-protein-coupled receptor[2] now referred to as UT receptor. The human (h) U-II precursor was cloned few years ago,[3] and the human prepro-U-II is processed to generate a mature form of 11 amino acid residues.[4] The U-II/UT receptor system seems to play an important role in cardiovascular functions; in fact, hU-II has been shown to be 1−2 orders of magnitude more potent than endothelin-1 in producing vasoconstriction in mammals and thus is one of the most effective vasoconstrictor compounds identified to date.[2,5,6] On the basis of its spectrum of activities, hU-II has been postulated to contribute as modulator to cardiovascular homeostasis and possibly to be involved in certain cardiovascular pathologies.[5,7] It has been recently demonstrated that U-II is involved in inhibition of insulin release[8] in the perfused rat pancreas and may play an important role in pulmonary hypertension.[9] Central nervous effects of U-II have also been described.[10] Hence, the hU-II antagonists could be of therapeutic value in a number of pathological disorders.

We have identified both a superagonist (P5U)[11] and an antagonist (urantide)[12] of hU-II. The latter is the most potent peptide antagonist at the UT receptor described to date.[12]

The conformational behavior of U-II has been previously described both in isotropic[13−15] and anisotropic environments.[16] Spectroscopic investigations indicated that in isotropic environments (water and DMSO solutions) the hexacyclic region is well-defined, although no classical secondary structure can be observed. Flohr et al.[14] described the particular structural arrangement of the Trp[7], Lys[8], and Tyr[9] triad, which resulted in being the key residues for the UT receptor interaction.[14,17−19] The pharmacophoric distances found in this NMR study[14] were then used in a successful virtual screening of a proprietary database. The search allowed the discovery of the first non-peptide UT antagonist named S6716. In the anisotropic membrane-like environment, hU-II and its analogues with agonist activity, among which is P5U, adopt a well-defined type II′ β-hairpin structure encompassing residues 5−10.[16] This structural arrangement allows a tight contact among Trp[7], Lys[8], and Tyr[9] side chains, which is fundamental to obtain full agonist activity. We have now synthesized, biologically evaluated, and analyzed by NMR and computational methods new U-II analogues with either partial-agonist or antagonist activity and compared their structures with that of P5U. The overall results allowed us to formulate a hypothesis about the structural changes that determine the switching from agonist to antagonist activity.

Results

Chemistry. Peptides were synthesized according to the solid-phase approach using standard Fmoc methodology in a manual reaction vessel[20] (Experimental Section).

The purification was achieved using a semipreparative RP-HPLC C18 bonded silica column (Vydac

* To whom correspondence should be addressed. Phone: +39-081-678646. Fax: +39-081-678644. E-mail: novellin@unina.it.
[§] University of Naples "Federico II".
[‡] These authors contributed equally to the work.
[†] Chiesi Pharmaceuticals S.p.A.
[||] Menarini Ricerche.
[#] Università di Firenze.

10.1021/jm058043j CCC: $30.25
Published on Web 10/14/2005

Table 1. Receptor Affinity and Biological Activity of Urotensin-II Analogues of General Formula R-Asp-c[Xaa-Phe-Yaa-Zaa-Tyr-Cys]-Val-OH[a]

peptide	Xaa	Yaa	Zaa	pK_i [b]	pEC$_{50}$ [c]	E_{max} (% hU-II)	pA_2 [d]
hU-II	Cys	Trp	Lys	9.1 ± 0.08	8.3 ± 0.06	100	
hU-II(4−11)	Cys	Trp	Lys	9.6 ± 0.07	8.6 ± 0.04	100	
P5U	Pen	Trp	Lys	9.7 ± 0.07	9.6 ± 0.07	97 ± 3	
1	Pen	D-Trp	Lys	8.9 ± 0.06	7.2 ± 0.04	33 ± 9	
2	Cys	D-Trp	Lys	8.9 ± 0.06	7.2 ± 0.04	42 ± 11	
3	Pen	Trp	Orn	7.8 ± 0.05	wa[e]	22 ± 6	7.4 ± 0.06
4	Cys	Trp	Orn	8.0 ± 0.06	wa[e]	36 ± 10	7.3 ± 0.08
5	Pen	D-Trp	Orn	8.3 ± 0.04	inactive		8.3 ± 0.09
6	Cys	D-Trp	Orn	7.9 ± 0.05	inactive		8.0 ± 0.06
7	D-Pen	D-Trp	Orn	5.7 ± 0.08	inactive		
8	Pen	D-Trp	D-Orn	6.4 ± 0.06	wa[e]	25 ± 7	

[a] R = H-Glu-Thr-Pro for hU-II; R = H for hU-II(4-11), P5U, and peptides **1**−**8**. [b] pK_i = −log K_i. [c] pEC$_{50}$ = −log EC$_{50}$. [d] pA_2 = −log A_2. Each value in the table is mean sem of at least four determinations. [e] wa = weak agonist.

218TP1010). The purified peptide was 98% pure as determined by analytical RP-HPLC. The correct molecular weight of the peptide was confirmed by mass spectrometry and amino acid analysis (Supporting Information).

Biological Data. Receptor affinity at the human UT receptor and biological activity (rat aorta bioassay) of the synthesized compounds are reported in Table 1. Compound **1**, which differs from P5U only for the D-Trp/L-Trp residue substitution at position 7, behaves as a partial agonist, with potency and efficacy greatly reduced when compared to P5U in the rat aorta bioassay (pEC$_{50}$ = 7.2 vs 9.6, $E_{max\%}$ = 33 vs 97). The related compound **2** (Cys5/Pen5) is also a partial agonist, possessing similar affinity, potency, and efficacy as **1**. Peptide **3**, which differs from P5U only for the Orn/Lys residue substitution at position 8, behaves as a competitive antagonist (pA_2 = 7.4), showing a small but consistent residual partial agonist activity. The related compound **4** (Cys5/Pen5) possesses a similar pharmacological profile as **3**; it also behaves as a partial agonist/antagonist. Urantide (**5**) behaves as competitive, potent (pA_2 = 8.3), and pure antagonist (no residual agonist activity up to 10 μM). The related compound **6** (Cys5/Pen5) also behaves as an antagonist with slightly reduced affinity and potency (pA_2 = 8.0) compared to **5**. Finally, peptides **7** and **8** both have low binding affinity and are virtually inactive either as agonist or as antagonist.

NMR Analysis in SDS Micelles. We have recently reported the NMR structure of UT agonists, among which P5U is the most potent peptide agonist at the UT receptor.[16] In micelles, the UT agonists showed a well-defined β-hairpin structure composed of a type-II′ β-turn with the Trp^7 residue in position i + 1, flanked by two short antiparallel strands. In this section, we analyze the diagnostic NMR parameters of some new analogues and compare them with the corresponding parameters in P5U.

A whole set of 1D and 2D NMR spectra in 200 mM aqueous solution of SDS were collected for compounds **1**, **3**, **5**, and **7**. These peptides were chosen on the basis of their sequence similarity and their broad range of biological activity (see above). To check for the absence of an aggregation state of the peptides, spectra were acquired in the concentration range of 0.2−5 mM. No significant changes were observed in the distribution and in the shape of the ^{1}H NMR resonances, indicating that no aggregation phenomena occurred in this concentration range. Complete ^{1}H NMR chemical shift assignments were effectively achieved for all the analyzed peptides according to the Wüthrich procedure[21] via the usual systematic application of DQF-COSY,[22] TOCSY,[23] and NOESY[24] experiments with the support of the XEASY software package (Supporting Information).[25]

Backbone Conformations. Peptide **1** differs from P5U only for the D-Trp/L-Trp residue substitution at position 7, and as expected, significant differences are observed in the NMR parameters of the changed residue. Diagnostic NMR parameters observed for the NH and H$_\alpha$ proton atoms of other residues (chemical shifts, NOE contacts, $^3J_{NH-H\alpha}$ coupling constants, NH exchange rates, and temperature coefficients) are all similar to those observed in P5U (Supporting Information). In particular, NOE contacts between H$_\alpha$−NH$_{i+2}$ of D-Trp^7 and Tyr^9 and between NH−NH$_{i+1}$ of Lys^8 and Tyr^9 indicated the presence of a β-turn. This result was supported by the observation of a slowly exchanging NH resonance of residue 9 and the low value of the temperature coefficient for this proton ($-\Delta\delta/\Delta T$ < 3.0 ppb/K). A short stretch of the antiparallel β-sheet involving residues 5 and 6 and residues 10 and 11 is inferred from a number of long-range NOEs including H$_\alpha$−NH connectivities between residues 5 and 11 and residues 10 and 6 and a NH−NH connectivity between residues 6 and 9. All the data indicated the preservation, in **1**, of the β-hairpin structure.

Peptide **3** differs from P5U only for the Orn/Lys residue substitution at position 8. The NMR parameters involving HN and H$_\alpha$ protons of **3** are very similar to the corresponding ones in P5U (Supporting Information). The data indicate a type II′ β-hairpin structure for **3**, as found for **1**, P5U, and other UT agonists. The major difference between the sets of NMR parameters involving the HN and H$_\alpha$ protons of **3** and P5U was the resonance value of the amide proton of Orn^8, which was shifted downfield from 6.60 (P5U) to 6.84 ppm (**3**).

The NMR parameters obtained for the NH and H$_\alpha$ proton atoms of **5** strictly resemble those of **1**, which shares all the sequences except the Orn/Lys homologous substitution at position 8. Again, all the data indicate the presence of a β-hairpin structure as in the previously described analogues. The major difference comparing backbone resonances of **5** and **1** was the downfield shift observed for the resonance of the NH of Orn^8, which shifted from 6.58 (**1**) to 7.22 ppm (**5**).

Table 2. Side Chain χ_1 Rotamers[a] and $^3J_{H\alpha-H\beta}$ Coupling Constants[b] of Cyclic Residues[c]

	Phe^6 $J_{\alpha\beta(l)}-J_{\alpha\beta(h)}$;[f] t, g$^-$, g$^+$ [g]	(D/L)-Trp^7 [d] $J_{\alpha\beta(l)}-J_{\alpha\beta(h)}$;[f] t, g$^-$, g$^+$ [g]	Lys^8 [e] $J_{\alpha\beta(l)}-J_{\alpha\beta(h)}$;[f] t, g$^-$, g$^+$ [g]	Tyr^9 $J_{\alpha\beta(l)}-J_{\alpha\beta(h)}$;[f] t, g$^-$, g$^+$ [g]
P5U	9.7−5.6; 60, 20, 20	11.5−5.0; 77, 14, 9	3.4−7.2; 7, 42, 51	5.6−9.9; 20, 62, 18
1	9.8−5.5; 61, 19, 20	11.3−5.2; 75, 9, 16	3.3−7.2; 6, 42, 52	5.7−9.8; 21, 61, 18
3	9.1−5.8; 54, 22, 24	8.5−7.4; 48, 37, 13	3.6−7.4; 9, 44, 45	5.5−9.7; 19, 60, 21
5	9.0−6.0; 53, 24, 23	8.5−7.8; 48, 11, 41	3.3−7.2; 6, 42, 52	5.4−9.9; 18, 62, 20
7	8.6−7.4; 49, 37, 12	11.0−5.8; 72, 6, 22	7.7−6.0; 47, 31, 22	7.6−6.8; 40, 32, 28

[a] Rotamer populations were calculated using $J_T = 13.56$ and $J_G = 2.60$ for nonaromatic side chains,[27a] while for aromatic side chain coupling constants required for the analysis were set to 13.85 and 3.55.[27b] Antiperiplanar trans and gauche rotamers were distinguished as reported in ref 27c. [b] Coupling constants are reported in Hz. [c] The degeneracy of the H resonances of Cys^{10} does not allow us to calculate the rotamer populations. [d] The most populated rotamers of (D/L)-Trp^7 are evidenced. [e] Orn^8 for **3** and **5**. [f] The subscripts (l) and (h) denote the coupling constant of the low- and high-field H signal, respectively. [g] *t*, *g*$^-$, and *g*$^+$: population percentage of the relevant rotamer.

Several spectral features of the inactive analogue **7** indicate a different conformational behavior of this peptide compared to the other described above and to P5U. In particular, the peptide shows significant differences in the NH and H_α resonances compared to all the other analyzed compounds (Supporting Information). The variation of the H_α resonances indicates a different backbone disposition.[26] The $H_\alpha-NH_{i+2}$ connectivity between D-Trp^7 and Tyr^9 indicates the presence of a β-turn about these residues. This result was supported by the observation of slowly exchanging NH resonance of Tyr^9 and the low value of the temperature coefficient for this proton ($-\Delta\delta/\Delta T$ < 3.0 ppb/K). The absence of interstrain NOEs and the $^3J_{NH-H\alpha}$ coupling constant values of the residues flanking the turn region (6 Hz < $^3J_{NH-H\alpha}$ < 8 Hz) indicate the loss of the ordered strand regions.

Side Chains Conformation. Major χ_1 Rotamers. Side chain orientations of the analyzed analogues were estimated by employing the rotational isomeric state approximation.[27] According to this model, an equilibrium exists among three side chain rotamers with χ_1 angle values of −60° (gauche$^-$, g$^-$), +180° (trans), and +60° (gauche$^+$, g$^+$). In Table 2 the obtained χ_1 rotamer populations are reported along with the experimental $^3J_{H\alpha-H\beta}$ coupling constants used in the calculation. Considering the high-affinity ligands P5U, **1**, **3**, and **5**, very similar results were obtained for all the residue side chain orientations except for that of residue 7. In particular, Phe^6, Lys^8 (Orn^8), and Tyr^9 side chains showed a large preference for trans, g$^+$/g$^-$, and g$^-$ rotamers, respectively. Considering the residue 7 side chain, while the agonist P5U and the partial agonist **1** show a large prevalence of the trans rotamer, the partial agonist/antagonist **3** and the pure antagonist **5** show a higher degree of flexibility of this side chain with an increased population of g$^-$ and g$^+$ rotamers, respectively (in D-type residues, the g$^+$ rotamer corresponds to the g$^-$ rotamer of the L-type residues). As a consequence, in the two last analogues, the (D/L)-Trp7 side chain is further from the Orn^8 and Tyr^9 side chains. This result agrees with the observed NOE contact patterns and also with the upfield shift of Lys^8 NH proton resonance observed for P5U and **1** (see above), which is probably due to the influence of the (D/L)-Trp^7 ring current on this proton resonance.

Peptide **7** shows a prevalence of the trans rotamer at the D-Trp^7 side chain, but the side chains of residues Phe^6, Orn^8, and Tyr^9 are less defined (Table 2). The loss of NOE contacts of Orn^8 with both D-Trp^7 and Tyr^9 side chain proton resonances confirms this high flexibility.

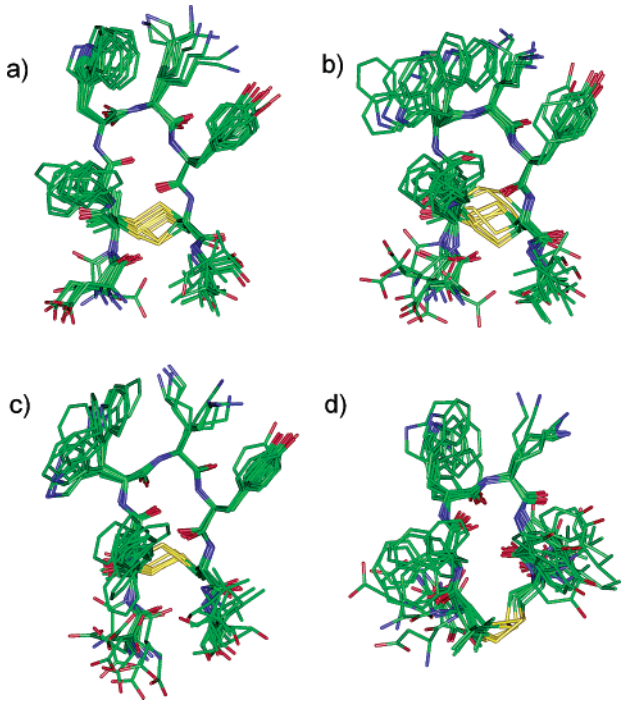

Figure 1. Superposition of the 10 lowest energy conformers of **1** (a), **3** (b), **5** (c), **7** (d). Structures were superimposed using the backbone heavy atoms of residues 5−10. Heavy atoms are shown with different colors (carbon, green; nitrogen, blue; oxygen, red; sulfur, gold). Hydrogen atoms are not shown for clarity.

Peptide Structure Calculations. NMR-derived constraints obtained for the analyzed peptides were used as the input data for a simulated annealing structure calculation as described in the Supporting Information. For each peptide, 20 calculated structures satisfying the NMR-derived constraints (violations smaller than 0.20 Å) were chosen (Figure 1). In Figure 1a−c, the UT receptor high-affinity ligands **1**, **3**, and **5** show a well-defined β-hairpin structure encompassing residues 5−10 (rmsd values are reported in the Supporting Information). Mainly, the side chain orientation is also well-defined with the exception of the (D/L)-Trp^7 side chain of both **3** (Figure 1b) and **5** (Figure 1c), in accordance with the low number of constraints observed for these side chains. On the basis of the χ_1 angle value of (D/L)-Trp^7, two families of structures (trans and gauche) can be defined for **3** and **5**. For **3**, $^{11}/_{20}$ structures belong to the trans family (named 3t, $\chi_1 = 180 \pm 20°$) and $^9/_{20}$ belong to the g$^-$ family (named 3g, $\chi_1 = -60 \pm 20°$). For **5**, we observed $^{10}/_{20}$ structures both for the trans (named 5t, $\chi_1 = 180 \pm 20°$) and for the g$^+$ (named 5g, $\chi_1 = 60 \pm 20°$) families. These population ratios are

in good accordance with those found above using the rotational isomeric state approximation.

Peptide **7** (Figure 1d) possesses a less defined structure. It loses the β-hairpin structure characteristic of high-affinity ligands. In particular, the N- and C-terminal residues show very different orientations when compared to the other analogues, which is due to the inversion of the configuration at the Pen^5 C_α atom. The β-II′ turn structure is still observable, but the Orn^8 and Tyr^9 side chain orientations are poorly defined, and the D-Trp^7 side chain, which shows a preferred trans orientation, occupies a different spatial position compared to the agonist P5U, mainly as consequence of the different value of the χ_2 angle ($-81 \pm 30°$ in **7** vs $+30 \pm 10$ in P5U).

Discussion

We have synthesized, biologically evaluated, and studied the conformational properties of various analogues of U-II (Table 1). SAR studies indicate that the replacement of the Trp^7 residue with the corresponding D-isomer switches the activity from agonist to partial agonist.[14,17−19,28] Similarly, partial agonists are obtained by replacement of the Lys^8 residue with Orn; however, in this case a weak antagonist activity is also observed.[19,29] The simultaneous presence of a D-Trp residue in position 7 and an Orn residue in position 8 leads to a potent antagonist devoid of any residual agonist activity (urantide, **5**).[12] The substitution of the Cys^5 with Pen enhances the agonist potency (hU-II(4−11)/P5U)[11] in the analogues bearing the L-Trp residue in position 7 while bringing about only minor effects, if any, on partial agonists and antagonists, thus indicating that the stabilization of the type II′ β-hairpin structure is important for triggering the biological response upon occupation of the receptor.

The partial agonist **1**, the partial agonist/antagonist **3**, the pure antagonist **5**, and the inactive compound **7** were subjected to extensive conformational analysis. The NMR analyses were performed in a membrane mimetic environment (SDS solution), since we have previously succeeded in correlating the micelle-bound structure of UT agonists to their activity.[16]

The analyzed analogues that retain high affinity for UT receptor (i.e., **1**, **3**, and **5**) all possess a type II′ β-hairpin backbone conformation as P5U,[16] regardless of their agonist or antagonist activity, indicating that such backbone conformation is necessary for the UT recognition. The inactive compound **7** did not show any propensity to hairpin formation. This result, together with a different orientation of the pharmacophoric side chains, can explain the inactivity of the peptide.

The main conformational difference observed in the structures of the antagonists **5** and **3** and the agonists P5U[16] and **1** consists of a different orientation of the (D/L)-Trp^7 side chain. In particular, while in P5U and **1** (Table 2 and Figure 1) the side chain of (D/L)-Trp^7 adopts a well-defined trans orientation ($\chi_1 \approx 180°$), in **3** and **5** the (D/L)-Trp^7 side chain is more flexible with an increased amount of the gauche population. For both **3** and **5**, two families of structures can be defined (3g and 3t for **3**; 5g and 5t for **5**) based on the different orientation of the (D/L)-Trp^7 side chain. In Table 3, the distances among the putative pharmacophoric points according to Fhlor et al.[14] are reported. The different conformational behavior of UT antagonists vs agonists prompted us to hypothesize that the different side chain orientation of the (D/L)-Trp^7, together with the Lys/Orn substitution at position 8, represents the structural basis for the agonist/antagonist activity switching observed in our compounds. In Figure 2, a superposition of representative structures of P5U and urantide 5g family is shown. Clearly, while in the agonist a tight contact among the Trp^7, Lys^8, and Tyr^9 side chains is observed in the antagonist, the D-Trp indole moiety is far from the Orn^8 and Tyr^9 side chains. As consequence of our structural hypothesis, pharmacophoric distances observed in the 5g family (Table 3) can be considered as a model for the UT antagonist queries.

The distances between the putative pharmacophoric points were already reported by Flohr et al.[14] for U-II and [D-Trp^7]U-II. These distances were used as input for a virtual screening of a proprietary database. The search performed with the U-II pharmacophoric distances allowed the discovery of new non-peptide antagonists. Interestingly, the U-II pharmacophoric distances found by Flohr are similar to those found in our antagonist model (Table 3).

Table 3. UT-II Receptor Ligand Pharmacophoric Distances (Å)

peptide	Trp^7 [b]−Lys^8 [c] Nϵ	Trp^7 [b]−Tyr^9 [b]	Lys^{8}Nϵ−Tyr^9 [b]
P5U	5.6	6.1	6.2
1	6.5	8.9	6.3
3g	8.5	10.4	5.0
3t	4.7	7.9	4.8
5g	9.1[d]	11.5	5.4
5t	5.6	9.4	7.1
7	7.2	11.2	9.0
U-II[e]	11.3	12.2	6.4

[a] Reported distances were measured as the mean of the 20 calculated structures of P5U, **1**, and **7**, while for **3** and **5** two subfamilies of structures (3g and 3t for **3**; 5g and 5t for **5**) were considered (see text). [b] Aryl ring centroids. [c] Orn^8 in **3**, **5**, and **7**. [d] Distances of the hypothesized antagonist model are evidenced. [e] Distances reported in ref 14.

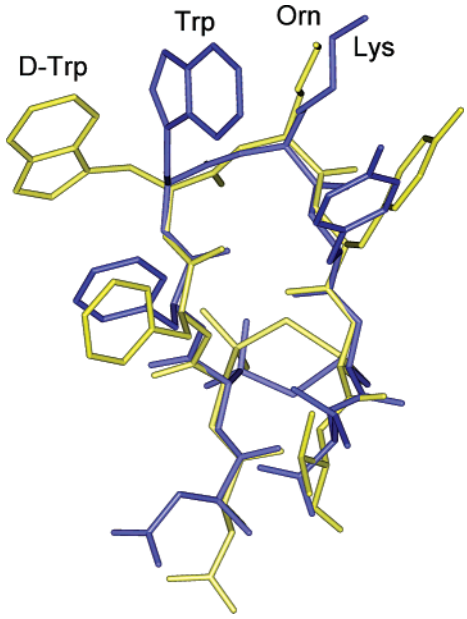

Figure 2. Superposition of representative structures of P5U (blue) and urantide (yellow). Structures were superimposed using the backbone heavy atoms of residues 5−10. Hydrogen atoms are not shown for clarity.

The NMR-derived structures of the analyzed compounds could explain their relative biological activities and receptor affinities (Table 1). Starting from the structure of the full agonist P5U,[16] the analogue **1** shows very similar conformational preferences considering both the backbone and side chain dispositions. The reduced agonist activity of **1** relative to P5U can be attributed to the increased distances between the D-Trp^7 indole moiety and the N_ζ of the Lys^8 and between the D-Trp^7 indole moiety and the phenol ring of the Tyr^9 observed in the first (Table 3). The antagonist activity of compound **3** can be attributed to its g^- conformer, which shows pharmacophore distances similar to those in 5g (Table 3). In contrast, the residual agonist activity can be attributed to the trans conformer, in which pharmacophoric distances resemble those observed in P5U. The antagonist **5** also shows a trans/gauche equilibrium at the D-Trp^7 side chain. The increased pA_2 value, compared to that for **3**, could be attributed to the increased gauche population and/or to a better fit to the antagonist ideal distances between the pharmacophoric points. On the other hand, the potential agonist activity of the trans form is completely (or almost completely; see below) abolished by the Lys/Orn substitution and by nonfitting distances to the agonist pharmacophore model (Table 3).

Regoli et al. have recently reported that urantide (**5**) shows agonist activity in a calcium mobilization assay performed in CHO_{hUT} cells.[30] Therefore, **5** behaves as a pure antagonist in the rat aorta bioassay and as a full agonist in $[Ca^+]_i$ mobilization assay performed on cells expressing the hUT. Hence, the potential use of urantide as antagonist lead compound at the human UT receptor has been largely debated. The results obtained by Camarda et al.[30] showing that urantide behaves as an agonist at transfected hUT receptor hosted in CHO cells hamper the compound from being classified as a "pure" antagonist. Indeed, this latter category implies a null efficacy in stimulating a given receptor. However, it should be noted that a relevant difference exists between the rat isolated aorta assay on one hand and the human recombinant receptor expressed by CHO cells on the other. As the same authors had described in a previous investigation,[31] the rat isolated thoracic aorta is by far the most responsive assay (among a wide variety of animal or human organs) to urotensin II probably because the thoracic aorta is particularly enriched with UT receptors compared to other vessels or even compared to the abdominal tract of the same vessel.[7] Therefore, our finding that urantide is devoid of any agonist activity in the thoracic aorta[12] is strongly predictive of lack of agonist behavior of this compound in vivo. Accordingly, the agonist/antagonist behavior of urantide was attributed to the different efficiency of the stimulus-response coupling that characterizes the rat aorta and $[Ca^+]_i/CHO_{hUT}$ assays, being low for the former and very high for the latter.[30] Thus, the efficacy of **5** is overestimated in the cell system expressing high levels of recombinant receptor,[29] while in the rat aorta, where the density of UT sites is relatively low,[2] the efficacy of **5** cannot be detected.

A second possibility exists to accommodate our[12] and Camarda's[30] data, that is, the existence of species differences between rat and human UT receptors. In fact, these two receptors share only ~75% of the homology[2] and the U-II sequence encompasses 11 and 14 amino acid residues, respectively. Furthermore, a recent study has demonstrated that the U-II peptide analogue SB-710411 exerts an antagonistic effect at the recombinant rat U-II receptor and acts as a full agonist at the recombinant monkey U-II receptor.[32] The discrepancies between the biological responses observed with the rat aorta paradigm and the $[Ca^+]_i$ mobilization assay were already pointed out by Brkovic et al.[18] Anyway, some lines of evidence make this second hypothesis unlikely, as widely discussed by Camarda and co-workers.[30] The lack of information about the effects of urantide in humans leaves it as an open question.

If the first hypothesis was valid, i.e., urantide behaves as antagonist also at human UT receptor, its agonist activity in $[Ca^+]_i/CHO_{hUT}$ assays would be attributable to the D-Trp^7 trans rotamer population, which is still observable in this compound. To discriminate between the two hypotheses and to further support our agonist/antagonist structural model, we are now developing new analogues of urantide (**5**) in which the D-Trp^7 side chain is conformationally restrained to the g^+ orientation.

Conclusions

In conclusion, a type II′ β-hairpin structure was a common feature found in both agonist and antagonist peptides acting on the UT receptor, indicating that such backbone conformation is necessary for the UT recognition. The main difference observed between the structures of the peptide antagonists, such as urantide (**5**), and the agonists, such as P5U, consists of a different preferred orientation of the (D/L)-Trp^7 side chain. In particular, while in P5U and related agonists the side chain of (D/L)-Trp^7 adopts a trans orientation, in urantide the D-Trp^7 side chain is more flexible with an increased amount of the g^+ rotamer population. We therefore hypothesize that the different side chain orientation of the Trp^7 indole moiety and the Lys/Orn substitution at position 8 represents the structural basis for the agonist/antagonist activity switching observed in our compounds. This investigation offers a precise model for the design of novel peptide and non-peptide antagonists to be used as pharmacological probes in revealing the (patho)physiological role of U-II and with potential antihypertensive and heart failure protective activities.

Experimental Section

Synthesis. N^α-Fmoc-protected amino acids, HBTU, and HOBt were purchased from Inbios (Naples, Italy). Wang resin was purchased from Advanced ChemTech (Louisville, KY). Protected Pen was purchased from Bachem (Basel, Switzerland). Peptide synthesis solvents, reagents, and CH_3CN for HPLC were reagent grade and were acquired from commercial sources and used without further purification unless otherwise noted. The synthesis of hU-II analogues was performed in a stepwise fashion via the solid-phase method. N^α-Fmoc-Val-OH was coupled to Wang resin (0.5 g, 0.7 mmol of NH_2/g). The following protected amino acids were then added stepwise: N^α-Fmoc-Cys(Trt)-OH, N^α-Fmoc-Tyr(OtBu)-OH, N^α-Fmoc-Zaa(N^ϵ-Boc)-OH (Zaa = Lys, Orn, DOrn), N^α-Fmoc-Yaa(N^{in}-Boc)-OH (Yaa = Trp, DTrp), N^α-Fmoc-Phe-OH, N^α-Fmoc-Xaa(Trt)-OH (Xaa = Cys, Pen, DPen), and N^α-Fmoc-Asp(OtBu)-OH. Each coupling reaction was accomplished using a 3-fold excess of amino acid with HBTU and HOBt in the presence of DIEA.

The N^{α}-Fmoc protecting groups were removed by treating the protected peptide resin with a 25% solution of piperidine in DMF (1 × 5 min and 1 × 20 min). The peptide resin was washed three times with DMF, and the next coupling step was initiated in a stepwise manner. All reactions were performed under an Ar atmosphere. The peptide resin was washed with DCM (3×), DMF (3×), and DCM (4×), and the deprotection protocol was repeated after each coupling step. The N-terminal Fmoc group was removed as described above, and the peptide was released from the resin with TFA/Et_3SiH/H_2O (90:5:5) for 3 h. The resin was removed by filtration, and the crude peptide was recovered by precipitation with cold anhydrous ethyl ether to give a white powder that was purified by RP-HPLC on a semipreparative C18-bonded silica column (Vydac 218TP1010, 1.0 cm × 25 cm) using a gradient of CH_3CN in 0.1% aqueous TFA (from 10% to 90% in 45 min) at a flow rate of 1.0 mL/min. The product was obtained by lyophilization of the appropriate fractions after removal of the CH_3CN by rotary evaporation. Analytical RP-HPLC indicated a purity >98%, and molecular weights were confirmed by FAB-MS (Fisons model Prospec) or HR-MS (Kratos Analytical model Kompact) (Supporting Information).

General Method of Oxidation and Cyclization. The peptides were oxidized by the syringe pump method previously reported.[33] The linear peptide (300−500 mg) was dissolved in 40 mL of 50% H_2O/25% acetonitrile/25% methanol, and nitrogen gas was passed through the solution for 20 min. An amount of 5 mL of saturated ammonium acetate solution was added, and the pH was taken to 8.5 with NH_4OH. The peptide solution was then added at room temperature via syringe pump to a stirred oxidant solution. The oxidant solution was prepared as follows. An amount of 2 equiv of potassium ferricyanide was dissolved in 400 mL of H_2O/200 mL of acetonitrile/200 mL of methanol. To this solution was added 100 mL of saturated ammonium acetate, and the pH was then taken to 8.5 with NH_4OH. The peptide solution was added at such a rate that approximately 10 mg of peptide was delivered per hour per liter of the oxidant. After the addition of peptide was complete, the reaction mixture was stirred for an additional 5−6 h and then taken to pH 3.5 with glacial acetic acid. Amberlite IRA-68 (Cl form) was added to remove the iron ions, and the solution was stirred for 20 min and then filtered. The solution was concentrated using a rotary evaporator at 30 °C and then lyophilized. The material thus obtained was dissolved in glacial acetic acid, filtered to remove inorganic salts, and relyophilized. The crude cyclic peptides were purified by preparative HPLC on the system described above, using a gradient of 100% buffer for 20 min, then 0−20% acetonitrile in 5 min, followed by 20−60% acetonitrile in 40 min, all at 40 mL/min. Again, the peptides eluted near 50% organic/50% buffer. The purity of the cyclic peptides was checked by analytical HPLC (C-18 column, Vydac 218TP104, 4,6 mm × 25 cm), using a Shimadzu SPD 10A vp with detection at 230 and 254 nm and by TLC in four solvent systems in silica gel with detection by UV light, iodine vapors, and ninhydrin. The analytical data of the compounds synthesized in this paper are given in the Supporting Information.

Organ Bath Experiments. Male albino rats (Wistar strain, 275−350 g) were decapitated under ether anesthesia. The thoracic aorta was cleared of surrounding tissue and excised from the aortic arch to the diaphragm. From each vessel, a helically cut strip was prepared, and then it was cut into two parallel strips. The endothelium was removed by gently rubbing the vessel intimal surface with a cotton-tip applicator. The effectiveness of this maneuvre was assessed by the loss of relaxation response to acetylcholine (1 μM) in noradrenaline (1 μM) precontracted preparations. All preparations were placed in 5 mL organ baths filled with oxygenated normal Krebs−Henseleit solution. Motor activity of the strips was recorded isotonically (load 5 mN). A cumulative concentration−response curve to hU-II was constructed on one of the two strips, which served as control. The other strip received the antagonist peptide under examination, and after a 30 min incubation period, hU-II was administered cumulatively. Maximal contractile responses of preparations were obtained by administration of KCl (80mM) at the end of the cumulative curves to hU-II. Antagonist activity was expressed in terms of pK_B (negative logarithm of the antagonist dissociation constant) and, assuming a slope of −1.0, was estimated as the mean of the individual values obtained with the equation pK_B = log[(dose ratio) −1] − log[antagonist concentration].[34] Competitive antagonism was checked by the Schild plot method; a plot with linear regression line and slope not significantly different from unity was considered as proof of simple reversible competition.[34] Ethical approval of the experimental protocol with animals was obtained from the local ethics committee.

Binding Experiments. All experiments were performed on membranes obtained from stable CHO-K1 cells expressing the recombinant human UT receptor (Euroscreen ES-440-M, Bruxelles, Belgium). Assay conditions were the following: buffer Tris (20 mM, pH 7.4 at 37 °C) added with $MgCl_2$ (5 mM) and 0.5% BSA. Final assay volume was 0.1 mL, containing 1 μg of membrane proteins. The radioligand used for competition experiments was [^{125}I]urotensin II (specific activity 2000 Ci/mmol; Amersham Biosciences, Buckinghamshire, U.K.) in the range 0.07−1.4 nM (corresponding to 1/10 to 1/5 of its K_D). Nonspecific binding was determined in the presence of 1 μM unlabeled hU-II and ranged between 10% and 20% of total binding. The incubation period (120 min at 37 °C) was terminated by rapid filtration through Whatman GF/B filter sheets (presoaked in BSA 0.5% for 3 h). Filters were then washed four times with 4 mL of ice-cold Tris buffer (20 mM). Trapped radioactivity was counted by a Cobra (Canberra-Packard) γ-counter.

NMR Sample Preparation. The 99.9% ^2H_2O was obtained from Aldrich (Milwaukee, WI), 98% SDS-d_{25} was obtained from Cambridge Isotope Laboratories, Inc. (Andover, MA), and [(2,2,3,3-tetradeuterio-3-(trimethylsilanyl)]propionic acid (TSP) was obtained from MSD Isotopes (Montreal, Canada).

NMR Spectroscopy. The samples for NMR spectroscopy were prepared by dissolving the appropriate amount of peptide in 0.45 mL of ^1H_2O (pH 5.5), 0.05 mL of ^2H_2O to obtain a concentration 1−2 mM of peptides, and 200 mM of SDS-d_{25}. NH exchange studies were performed dissolving peptides in 0.50 mL of ^2H_2O and 200 mM of SDS-d_{25}. NMR spectra were recorded on a Varian INOVA 700 MHz spectrometer equipped with a z-gradient 5 mm triple-resonance probe head. All the spectra were recorded at a temperature of 300 K. The spectra were calibrated relative to TSP (0.00 ppm) as internal standard. One-dimensional (1D) NMR spectra were recorded in the Fourier mode with quadrature detection. The water signal was suppressed by the hard pulse WATERGATE scheme. 2D DQF-COSY,[22] TOCSY,[23] NOESY,[24] and PE COSY[35] spectra were recorded in the phase-sensitive mode using the method from States.[36] Data block sizes were 4096 addresses in t_2 and 512 equidistant t_1 values. Before Fourier transformation, the time domain data matrices were multiplied by shifted $\sin^2$ functions in both dimensions. A mixing time of 70 ms was used for the TOCSY experiments. NOESY experiments were run with mixing times in the range of 150−300 ms. The qualitative and quantitative analyses of DQF-COSY, PE COSY, TOCSY, and NOESY spectra were obtained using the interactive program package XEASY.[25] $^3J_{HN-H\alpha}$ coupling constants were obtained from 1D ^{1}H NMR and 2D DQF-COSY spectra. $^3J_{H\alpha-H\beta}$ coupling constants were obtained from 1D ^{1}H NMR and 2D PE-COSY spectra, the last performed with a β flip angle of 35°. The temperature coefficients of the amide proton chemical shifts were calculated from 1D ^{1}H NMR and 2D DQF-COSY experiments performed at different temperatures in the range 300−320 K by means of linear regression.

Structural Determinations and Computational Modeling. The NOE-based distance restraints were obtained from NOESY spectra collected with a mixing time of 200 ms. The NOE cross-peaks were integrated with the XEASY program and were converted into upper distance bounds using the CALIBA program incorporated into the program package DYANA.[37] Cross-peaks that were overlapped more than 50%

were treated as weak restraints in the DYANA calculation. In the first step, only NOE derived constraints (Supporting Information) were considered in the annealing procedures. For each examined peptide, 200 structures were generated with the simulated annealing of the program DYANA. An error-tolerant target function (tf type = 3) was used to account for the peptide intrinsic flexibility. Nonstandard Pen, D-Trp, and Orn residues were added to the DYANA residue library using MOLMOL.[38] From these structures we could univocally determine the hydrogen bond atom acceptors corresponding to the slowly exchanging NHs previously determined for each peptide. In a second DYANA run these hydrogen bonds were explicitly added as upper and lower limit constraints (NH of Phe^6 with CO of Tyr^9; NH of Tyr^9 with CO of Phe^6 for **1**, **3**, and **5**; NH of Tyr^9 with CO of Phe^6 for **7**), together with the NOE derived upper limit constraints (Supporting Information). The second annealing procedure produced 200 conformations from which 50 structures were chosen, whose interprotonic distances best fitted NOE derived distances, and then refined through successive steps of restrained and unrestrained EM calculations using the Discover algorithm (Accelrys, San Diego, CA) and the consistent valence force field (CVFF)[34] as previously described.[16] The minimization lowered the total energy of the structures; no residue was found in the disallowed region of the Ramachandran plot. The final structures were analyzed using the InsightII program (Accelrys, San Diego, CA). Graphical representation were carried out with the InsightII program (Accelrys, San Diego, CA). The rms deviation analysis between energy-minimized structures were carried out with the program MOLMOL.[38] The PROMOTIF program was used to extract details on the location and types of structural secondary motifs.[40]

Appendix

Abbreviations. Abbreviations used for amino acids and designation of peptides follow the rules of the IUPAC-IUB Commission of Biochemical Nomenclature in *J. Biol. Chem.* **1972**, *247*, 977−983. Amino acid symbols denote L-configuration unless indicated otherwise. The following additional abbreviations are used: U-II, urotensin II peptide; hU-II, human urotensin II peptide; SDS, sodium dodecyl sulfate; SAR, structure−activity relationship; NMR, nuclear magnetic resonance; DQF-COSY, double quantum filtered correlated spectroscopy; PE COSY, primitive exclusive correlated spectroscopy; TOCSY, total correlated spectroscopy; NOESY, nuclear Overhauser enhancement spectroscopy; NOE, nuclear Overhauser effect; MD, molecular dynamics; EM, energy minimization; 1D, 2D, and 3D, one-, two- and three-dimensional; Pen, pennicillamine; TSP, 3-(trimethylsilanyl)propionic acid; Orn, ornitine.

Supporting Information Available: Analytical data of the synthesized peptides, NMR data of the analyzed peptides, and rms deviations of the calculated structures. This material is available free of charge via the Internet at http://pubs.acs.org.

References

(1) Pearson, D.; Shively, J. E.; Clark, B. R.; Geschwind, I. I.; Barkley, M.; Nishioka, R. S.; Bern, H. A. Urotensin II: A Somatostain-like Peptide in the Caudal Neurosecretory System of Fishes. *Proc. Natl. Acad. Sci. U.S.A.* **1980**, *77*, 5021−5024.

(2) Ames, R. S.; Sarau, H. M.; Chambers, J. K.; Willette, R. N.; Aiyar, R. V.; Romanic, A. M.; Louden, C. S.; Foley, J. J.; Sauermelch, C. F.; Coatney, R. W.; Ao, Z.; Disa, J.; Holmes, S. D.; Stadel, J. M.; Martin, J. D.; Liu, W.-S.; Glover, G. I.; Wilson, S.; McNutty, D. E.; Ellis, C. E.; Eishourbagy, N. A.; Shabon, U.; Trill, J. J.; Hay, D. V. P.; Ohlstein, E. H.; Bergsma, D. J.; Douglas, S. A. Human Urotensin-II Is a Potent Vasoconstrictor and Agonist for the Orphan Receptor GPR14. *Nature* **1999**, *401*, 282−286.

(3) Coulouarn, Y.; Lihrmann, I.; Jegou, S.; Anouar, Y.; Tostivint, H.; Beauvillain, J. C.; Conlon, J. M.; Bern, H. A.; Vaudry, H. Cloning of the cDNA Encoding the Urotensin II Precursor in Frog and Human Reveals Intense Expression of the Urotensin II Gene in Motoneurons of the Spinal Cord. *Proc. Natl. Acad. Sci. U.S.A.* **1998**, *95*, 15803−15808.

(4) Chartrel, N.; Leprince, J.; Dujardin, C.; Chatenet, D.; Tollemer, H.; Baroncini, M.; Balment, R. J.; Beauvillain, J. C.; Vaudry, H. Biochemical Characterization and Immunohistochemical Localization of Urotensin II in the Human Brainstem and Spinal Cord. *J. Neurochem.* **2004**, *91*, 110−118.

(5) Maguire, J. J.; Davenport, A. P. Is Urotensin-II the New Endothelin? *Br. J. Pharmacol.* **2002**, *137*, 579−588.

(6) Douglas, S. A.; Ohlstein, E. H. Human Urotensin-II, the Most Potent Mammalian Vasoconstrictor Identified to Date, as a Therapeutic Target for the Management of Cardivascular Diseases. *Trends Cardiovasc. Med.* **2000**, *10*, 229−237.

(7) Douglas, S. A. Human Urotensin-II as a Novel Cardiovascular Target: "Heart" of the Matter or Simply a Fish "Tail"? *Curr. Opin. Pharmacol.* **2003**, *3*, 159−167.

(8) Silvestre, R. A.; Egido, E. M.; Hernandez, R.; Leprince, J.; Chatenet, D.; Tollemer, H.; Chartrel, N.; Vaudry, H.; Marco, J. Urotensin-II Is Present in Pancreatic Extracts and Inhibits Insulin Release in the Perfused Rat Pancreas. *Eur. J. Endocrinol.* **2004**, *151*, 803−809.

(9) Djordjevic, T.; Belaiba, R. S.; Bonello, S.; Pfeilschifter, J.; Hess, J.; Gorlach, A. Human Urotensin II Is a Novel Activator of NADPH Oxidase in Human Pulmonary Artery Smooth Muscle Cells. *Arterioscler. Thromb., Vasc. Biol.* **2005**, *25*, 519−525.

(10) Matsumoto, Y.; Abe, M.; Watanabe, T.; Adachi, Y.; Yano, T.; Takahashi, H.; Sugo, T.; Mori, M.; Kitada, C.; Kurokawa, T.; Fujino, M. Intracerebroventricular Administration of Urotensin II Promotes Anxiogenic-like Behaviors in Rodents. *Neurosci. Lett.* **2004**, *358*, 99−102.

(11) Grieco, P.; Carotenuto, A.; Campiglia, P.; Zampelli, E.; Patacchini, R.; Maggi, C. A.; Novellino, E.; Rovero, P. A New Potent Urotensin-II Receptor Peptide Agonist Containing a Pen Residue at Disulfide Bridge. *J. Med. Chem.* **2002**, *45*, 4391−4394.

(12) Patacchini, R.; Santicioli, P.; Giuliani, S.; Grieco, P.; Novellino, E.; Rovero, P.; Maggi, C. A. Urantide: An Ultrapotent Urotensin II Antagonist Peptide in the Rat Aorta. *Br. J. Pharmacol.* **2003**, *140*, 1155−1158.

(13) Bhaskaram, R.; Arunkumar, A. I.; Yu, C. NMR and Dynamical Simulated Annealing Studies on the Solution Conformation of Urotensin II. *Biochim. Biophys. Acta* **1994**, *1199*, 115−122.

(14) Flohr, S.; Kurz, M.; Kostenis, E.; Brkovich, A.; Fournier, A.; Klabunde, T. Identification of Nonpeptidic Urotensin II Receptor Antagonists by Virtual Screening Based on a Pharmacophore Model Derived from Structure−Activity Relationships and Nuclear Magnetic Resonance Studies on Urotensin II. *J. Med. Chem.* **2002**, *45*, 1799−1805.

(15) Grieco, P.; Carotenuto, A.; Patacchini, R.; Maggi, C. A.; Novellino, E.; Rovero, P. Design, Synthesis, Conformational Analysis, and Biological Studies of Urotensin II Lactam Analogues. *Bioorg. Med. Chem.* **2002**, *10*, 3731−3739.

(16) Carotenuto, A.; Grieco, P.; Campiglia, P.; Novellino, E.; Rovero, P. Unraveling the Active Conformation of Urotensin II. *J. Med. Chem.* **2004**, *47*, 1652−1661.

(17) Kinney, W. A.; Almond, H. R., Jr.; Qi, J.; Smith, C. E.; Santulli, R. J.; de Garavilla, L.; Andrade-Gordon, P.; Cho, D. S.; Everson, A. M.; Feinstein, M. A.; Leung, P. A.; Maryanoff, B. E. Structure−Function Analysis of Urotensin II and Its Use in the Construction of a Ligand−Receptor Working Model. *Angew. Chem., Int. Ed.* **2002**, *41*, 2940−2944.

(18) Brkovic, A.; Hattenberger, A.; Kostenis, E.; Klabunde, T.; Flohr, S.; Kurz, M.; Bourgault, S.; Fournier, A. Functional and Binding. Characterizations of Urotensin II-Related Peptides in Human and Rat Urotensin II-Receptor Assay. *J. Pharmacol. Exp. Ther.* **2003**, *306*, 1200−1009.

(19) Guerrini, R.; Camarda, V.; Marzola, E.; Arduin, M.; Calo, G.; Spagnol, M.; Rizzi, A.; Salvatori, S.; Regoli, D. Structure−Activity Relationship Study on Human Urotensin II. *J. Pept. Sci.* **2005**, *11*, 85−90.

(20) Stewart, J. M.; Young, J. D. In *Solid Phase Peptide Synthesis*; Pierce Chemical: Rockford, IL, 1984.

(21) Wüthrich, K. In *NMR of Proteins and Nucleic Acids*; John Wiley & Sons: New York, 1986.

(22) (a) Piantini, U.; Sorensen, O. W.; Ernst, R. R. Multiple Quantum Filters for Elucidating NMR Coupling Network. *J. Am. Chem. Soc.* **1982**, *104*, 6800−6801. (b) Marion, D.; Wüthrich, K. Application of Phase Sensitive Two-Dimensional Correlated Spectroscopy (COSY) for Measurements of $^1H-^1H$ Spin−Spin Coupling Constants in Proteins. *Biochem. Biophys. Res. Commun.* **1983**, *113*, 967−974.

(23) Bax, A.; Davis, D. G. Mlev-17-Based Two-Dimensional Homonuclear Magnetization Transfer Spectroscopy. *J. Magn. Reson.* **1985**, *65*, 355−360.

(24) Jenner, J.; Meyer, B. H.; Bachman, P.; Ernst, R. R. Investigation of Exchange Processes by Two-Dimensional NMR Spectroscopy. *J. Chem. Phys.* **1979**, *71*, 4546−4553.
(25) Bartels, C.; Xia, T.; Billeter, M.; Guentert, P.; Wüthrich, K. The Program XEASY for Computer-Supported NMR Spectral Analysis of Biological Macromolecules. *J. Biomol. NMR* **1995**, *6*, 1−10.
(26) Wishart, D. S.; Sykes, B. D.; Richards, F. M. The Chemical Shift Index: A Fast Method for the Assignment of Protein Secondary Structure through NMR Spectroscopy. *Biochemistry* **1992**, *31*, 1647−1651.
(27) (a) Pachler, K. G. R. Nuclear Magnetic Resonance Study of Some α-Amino Acids-II. Rotational Isomerism. *Spectrochim. Acta* **1964**, *20*, 581−587. (b) Cung, M. T.; Marraud, M. Conformational Dependence of the Vicinal Proton Coupling Constant for the Cα−Cβ Bond in Peptides. *Biopolymers* **1982**, *21*, 953−967. (c) Melacini, G.; Zhu, Q.; Goodman, M. Multiconformational NMR Analysis of Sandostatin (Octreotide): Equilibrium between β-Sheet and Partially Helical Structures. *Biochemistry* **1997**, *36*, 1233−1241.
(28) Chatenet, D.; Dubessy, C.; Leprince, J.; Boularan, C.; Carlier, L.; Segalas-Milazzo, I.; Guilhaudis, L.; Oulyadi, H.; Davoust, D.; Scalbert, E.; Pfeiffer, B.; Renard, P.; Tonon, M. C.; Lihrmann, I.; Pacaud, P.; Vaudry, H. Structure−Activity Relationships and Structural Conformation of a Novel Urotensin II-Related Peptide. *Peptides* **2004**, *25*, 1819−1830.
(29) Camarda, V.; Guerrini, R.; Kostenis, E.; Rizzi, A.; Calo, G.; Hattenberger, A.; Zucchini, M.; Salvatori, S.; Regoli, D. A New Ligand for the Urotensin II Receptor. *Br. J. Pharmacol.* **2002**, *137*, 311−314.
(30) Camarda, V.; Song, W.; Marzola, E.; Spagnol, M.; Guerrini, R.; Salvatori, S.; Regoli, D.; Thompson, J. P.; Rowbotham, D. J.; Behm, D. J.; Douglas, S. A.; Calo', G.; Lambert, D. G. Urantide Mimics Urotensin-II Induced Calcium Release in Cells Expressing Recombinant UT Receptors. *Eur. J. Pharmacol.* **2004**, *498*, 83−6.
(31) Camarda, V.; Rizzi, A.; Calo, G.; Gendron, G.; Perron, S. I.; Kostenis, E.; Zamboni, P.; Mascoli, F.; Regoli, D. Effects of Human Urotensin II in Isolated Vessels of Various Species; Comparison with other Vasoactive Agents. *Naunyn Schmiedeberg's Arch. Pharmacol.* **2002**, *365*, 141−149.
(32) Behm, D. J.; Herold, C. L.; Camarda, V.; Aiyar, N. V.; Douglas, S. A. Differential Agonistic and Antagonistic Effects of the Urotensin-II Ligand SB-710411 at Rodent and Primate UT Receptors. *Eur. J. Pharmacol.* **2004**, *492*, 113−116.
(33) Misika, A.; Hruby, V. J. Optimization of Disulfide Bond Formation. *Pol. J. Che*m. **1994**, *68*, 893−899.
(34) Kenakin, T. P. In *Pharmacologic Analysis of Drug−Receptor Interaction*; Lippincott-Raven: Philadelphia, PA, 1997.
(35) Mueller, L. P. E: COSY, a Simple Alternative to E. COSY. *J. Magn. Res.* **1987**, *72*, 191−196.
(36) States, D. J.; Haberkorn, R. A.; Ruben, D. J. A Two-Dimensional Nuclear Overhauser Experiment with Pure Absorption Phase in Four Quadrants. *J. Magn. Reson.* **1982**, *48*, 286−292.
(37) Guntert, P.; Mumenthaler, C.; Wüthrich, K.; Torsion Angle Dynamics for NMR Structure Calculation with the New Program DYANA. *J. Mol. Biol.* **1997**, *273*, 283−298.
(38) Koradi, R.; Billeter, M.; Wüthrich, K. MOLMOL: A Program for Display and Analysis of Macromolecular Structures. *J. Mol. Graphics* **1996**, *14*, 51−55.
(39) Maple, J.; Dinur, U.; Hagler, A. T. Derivation of Force Fields for Molecular Mechanics and Dynamics from ab Initio Energy Surface. *Proc. Natl. Acad. Sci. U.S.A.* **1988**, *85*, 5350−5354.
(40) Hutchinson, E. G.; Thornton, J. M. PROMOTIF—A Program To Identify and Analyze Structural Motifs in Proteins. *Protein Sci.* **1996**, *5*, 212−220.

JM058043J